Aalborg Universitet

AALBORG UNIVERSITY

DENMARK

Probabilistic RFID tag detector model

M. Jacobsen, Rasmus; Nielsen, Karsten Fyhn; Scaglione, Anna; Popovski, Petar; Larsen, Torben; Melchior Jacobsen, Rasmus

PROBABILISTIC RFID TAG DETECTOR MODEL

Rasmus M. Jacobsen[1], *Karsten F. Nielsen*[1], *Anna Scaglione*[2], *Petar Popovski*[1], *and Torben Larsen*[1]

[1]Aalborg University, Department of Electronic Systems, Denmark
[2]University of California, Davis, Department of Electrical and Computer Engineering, Davis, CA, USA
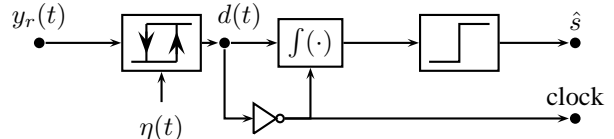
ABSTRACT

The objective of this paper is to derive the channel transition probabilities for the reader–to–tag link in RFID, considering the peculiar receiver structure in a RFID tag. The model is a first necessary step to derive Maximum Likelihood receivers and also the Shannon capacity of the link.
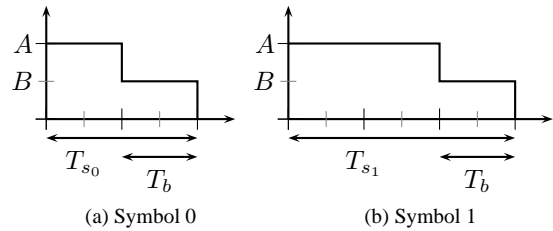
1. INTRODUCTION

The standardization and diffusion of RFID technology has prompted the introduction of various models and simulation platforms that describe its behaviour, see e.g. the popular RFIDsim [1]. Most platforms assume that the tag can be characterized with a simple bit error probability and do not accurately model the tag demodulation and decision process. One of the main characteristics in RFID is the simple passive tag structure, which have modest processing abilities, no local clock and is thus a non–coherent receiver.

The tag receiver structure uses a simple envelope detector circuit at the front–end. However, less common is the use of a clock–less analog to digital conversion: The sent data is Pulse Interval Encoded (PIE) [2], a special case of a Pulse Width Modulation (PWM) signal similar to e.g. Morse code, where the symbol information is in its *duration*. This allows for a clever form of detector circuit [3] which can be expressed as in Fig. 1, where the envelope is first processed by a trigger. The trigger thus changes state based on a threshold value $\eta(t)$ in the beginning and end of an on–pulse. The pulse from the trigger $d(t)$ can take values 0 or 1, depending on whether the envelope $y_r(t)$ is below or above $\eta(t)$, respectively. The pulse $d(t)$ is integrated, and the duration of the pulse is used to determine whether the symbol 0, 1 or no symbol was sent. The falling edge from the trigger is used to determine when to stop integrating, i.e. the discriminator makes its decision on the falling edge in a symbol. This is sufficient, as the area under $d(t)$ is represented by the time above $\eta(t)$ alone.

As mentioned, the information in PWM is encoded in the duration of an on–pulse, resulting in peculiar noise effects: Noise can merge or split symbols creating a sequence whose

The authors e–mails are: {raller,kfyhn,petarp,tl}@es.aau.dk, and ascaglione@ucdavis.edu. The first two authors are students on the AAU elite–programme, http://eliteeducation.aau.dk.

Fig. 1: Simple detector for PIE encoded data. [3]

(a) Symbol 0   (b) Symbol 1

Fig. 2: The PIE symbols.

length in general does not match the input sequence. This clarifies that the i.i.d. error model often assumed in RFID simulators is inaccurate and highlights the need of properly computing the channel transition probabilities, i.e. the probability of the output sequence given the input sequence. This is the objective of this paper and our derivations can be applied not only for simulation purposes but also to derive optimal Maximum Likelihood policies for the detection of the symbols, and Shannon capacity limits for this type of technology.

A model of the receiver structure is developed, describing the time/duration above $\eta(t)$ after an up–crossing. The signal representation used to model the duration is in Section 2, and a probabilistic model representing the duration is in Section 3. The work is concluded in Section 4.

2. SIGNAL REPRESENTATION

The two symbols in PIE are as depicted in Fig. 2. The durations T_{s_0} and T_{s_1} are decided by the reader prior to initiating any communication with tags. For simplicity, assume $T_{s_0} = 2T_b$ and $T_{s_1} = 3T_b$. In this way, each symbol s have the underlying bit–sequence $\ddot{s} = \{1, 0\}$ or $\ddot{s} = \{1, 1, 0\}$ for symbol 0 and 1, respectively. A PIE encoded message $M = \{s_0, s_1, \ldots, s_{S-1}\}$ is then a discrete sequence of bits,

this sequence is denoted p and follows from M as:

$$p = \{\ddot{\mathbf{s}}_0, \ddot{\mathbf{s}}_1, \ldots, \ddot{\mathbf{s}}_{S-1}\}.$$

This bit–sequence p is low–pass filtered at the reader with e.g. a raised cosine filter with cut–off factor 1 [4], resulting in the analog waveform $p_f(t)$, which satisfies the strict ripple requirements in the UHF band [5].

Assume a complex AWGN channel with path loss and the received signal at the tag is:

$$Y(t) = a \cdot p_f(t) + W(t),$$

where a is a real attenuation factor and $W(t)$ is band–limited noise. At the tag, to describe the probabilistic model of the duration, we now represent the signal $|Y(t)|$ as a function of its samples taken at the Nyquist rate. Given that the sampling grid is defined up to an arbitrary constant, for convenience, we consider samples that are perfectly aligned with the symbols, and assume that the channel does not introduce inter symbol interference. The tag does, however, not sample, it is rather a convenient abstraction for the analysis of the envelope. This then results in a sampled version of $|Y(t)|$: $X_k = |a \cdot p_k + W_k|$, where $W_k \sim \mathcal{N}_c\left(0, \frac{N_0}{2}\right)$. Now, let each envelope sample X_k be modelled by a Rician random variable $X_k \sim \text{Rice}\left(\frac{N_0}{4}, \mu_k\right)$ describing the envelope value $X_k = \sqrt{\Re(Y_k)^2 + \Im(Y_k)^2}$ where $\Re(Y_k) \sim \mathcal{N}\left(\mu_k, \frac{N_0}{4}\right)$ and $\Im(Y_k) \sim \mathcal{N}\left(0, \frac{N_0}{4}\right)$. This gives, that the data part of the signal at the tag is completely described by the samples:

$$\mathcal{X} = \{X_0, X_1, \ldots, X_k, \ldots, X_{S-1}\},$$

as all modulated information in PIE is amplitude modulated.

Introduce the index n in $\mathcal{X}$ to be the samples where $X_n < \eta$ and $X_{n+1} > \eta$, i.e. an up–crossing occurs between sample n and $n + 1$. There are multiple places in the sequence $\mathcal{X}$ where an up–crossing occurs, so n can take different values in the same sequence. It should be noted that n is not a–priori known at the tag, as the received noise affected sequence may contain adverse and misaligned crossings due to noise.

The mean values for the samples in $\mathcal{X}$, e.g. X_k with mean μ_k, corresponds uniquely to the transmitted bit p_k in p. A 0–bit in p corresponds to $\mu_k = \mu_{\text{under}}$ and 1–bit to $\mu_k = \mu_{\text{over}}$, where μ_{under} and μ_{over} are two mean values which are assumed constant during a symbol and a–priori known.

The threshold $\eta(t)$ may be a function of time on the tag (for example the average signal power) as the signal level may vary during a symbol, but in the following it is assumed that $\eta(t) = \eta$ is a–priori known and constant and that the signal level does not change during a symbol.

3. PROBABILISTIC MODEL OF PULSE DURATION

Introduce the random variable Z denoting the time above the threshold η, when the up–transition occurs between X_n and
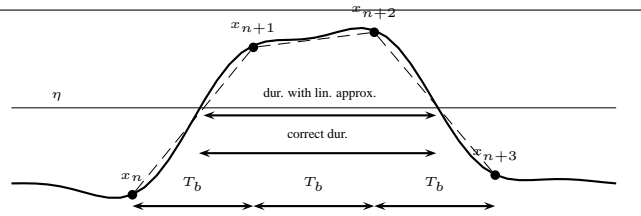

**Fig. 3**: The envelope and the linearly interpolated samples.

X_{n+1}. The conditional pdf for Z, $f(z|\bar{\bar{\mathbf{s}}}, X_n < \eta, X_{n+1} > \eta)$, shortened $f(z)$ for simplicity of notation, is derived in this section, where $\bar{\bar{\mathbf{s}}}$ is the mean sequence for the bits in a symbol, e.g. $\bar{\bar{\mathbf{s}}} = \{\mu_{\text{over}}, \mu_{\text{over}}, \mu_{\text{under}}\}$ for symbol 1. Let γ be the relative up–crossing time between the two samples x_n and x_{n+1}, i.e. the crossing occurred at time $nT_b + \gamma$. A convenient way to describe the band–limited behaviour between the samples is to introduce a 1st order linear approximation of the envelope between the samples in $\mathcal{X}$. That is, instead of analysing the threshold crossings on the envelope itself, analyse the up– and down–crossing on the linear interpolation between the samples.

Several authors (see e.g. [6]) have used the initial results in [7] to analyze level–crossing events for random processes, with the aim to get statistics about the average crossing rate of a random process using the joint pdf of the the random process and its derivative. In [6], also the conditional probability for a down–crossing given an up–crossing is found simililar to $f(z)$, however, the low–pass filtered process with varying mean depending on the transmitted symbol sequence considered in this work cannot be directly captured by these models.

3.1. Validity of Linear Approximation

To compare how the linear approximation affects the duration above η compared to the durations given by the actual envelope, consider the simulated setup where the example bit–sequences $p_{00} = \{1, 0, 1, 0\}$ and $p_{11} = \{1, 1, 0, 1, 1, 0\}$ corresponding to $M = \{0, 0\}$ and $M = \{1, 1\}$ respectively, are sent from the reader through the channel. The envelope is sampled at the tag, and the sample points are interpolated using both 1) the interpolation formula which completely reconstructs the envelope between the samples, and 2) the linear approximation where each sample is connected by a straight line. The following is an example for $\mu_{\text{over}} = 1.00442$, $\mu_{\text{under}} = 1$, $\eta = 1.00221$, $T_b = 5\mu s$, and a noise power $N_0 = -22$ dBm at the tag. The interpolation methods are for a symbol–1 in Fig. 3, where it can be seen that the choice of η affects the accuracy of the approximation. Assuming $\eta = \frac{\mu_{\text{over}} + \mu_{\text{under}}}{2}$, and the durations are almost equal.

In the comparison, the time of the up– and down–crossing is recorded to calculate the duration above η for the envelope and its approximation with linear interpolation. In Fig. 4 both normalized histograms are shown. In the example, it is clear that the two methods yield different results. This is mainly
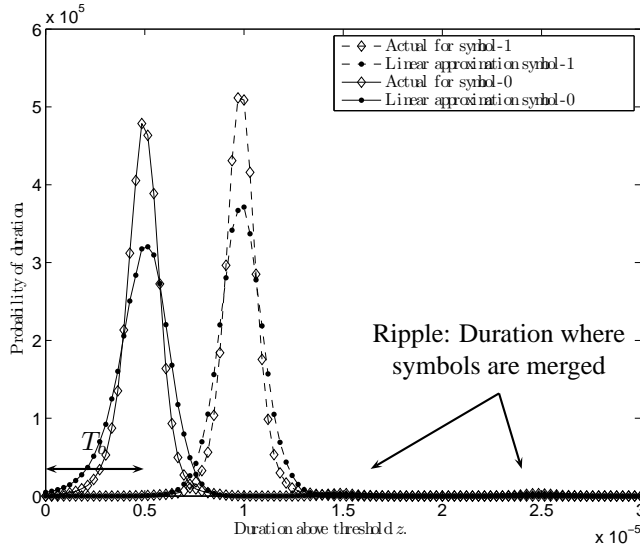
Fig. 4: Difference between correct duration and duration obtained using a linear approximation between sample points when p_{00} and p_{11} are sent. The histogram is normalized and based on 100.000 sequences sent through the channel.

because of the low SNR, however the shape of the approximation captures the channel effects, and the use of the approximation simplifies the sequel derivations. Future work should include better approximations.

3.2. A Note on Symbol Error–Types

The error–types arising can be seen by observing the histograms in Fig. 4. The ripples illustrates the event where the two transmitted 0–symbols (or 1–symbols) have merged into one long (unknown) symbol – this type of error arise when the last bit in a symbol is flipped. To capture these effects, it is not valid to approximate $f(z)$ with, for example, a simple Gaussian distribution. Also, by looking at the region $[T_b, 2T_b]$, these durations corresponds to the bit–sequence $\{1, 1, 0, x, x, x\}$, $\{1, 0, x, x, x, x\}$ or $\{0, 1, 0, x, x, x\}$, or a different bit–sequence making the types of symbol errors peculiar as they are not directly related with bit–errors. An analysis of error types and heuristics for optimizing the detector to mitigate the effect of the errors is the subject of future work.

3.3. Applying Linear Approximation

The approximation yields a relation between samples x_n, x_{n+1} and up–crossing time γ (similarly for the down–crossing). The slope from sample x_n through the threshold η onto x_{n+1} is uniquely determined by any two of x_n, x_{n+1} and γ:

$$x_{n+1} = \frac{(\eta - x_n)T_b}{\gamma} + x_n. \qquad (1)$$
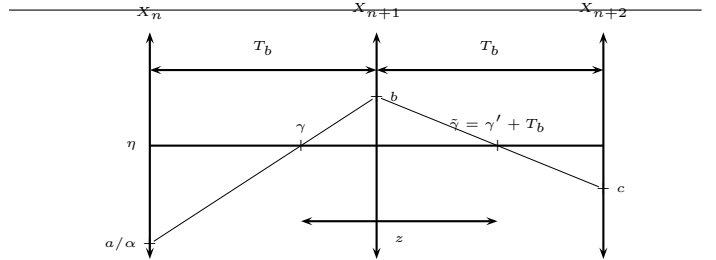
Fig. 5: Linear approximation applied between samples for Case A. The triplet $\{a, b, c\}$ depicted is one of the possible triplets yielding the same duration z.

The derivation of the pdf of the random duration Z is found by applying multidimensional random variable transformation [8] which maps the joint pdf of the random variables $X_n, X_{n+1}, \ldots$, into a joint transformed pdf $f_T(\alpha, \gamma, z)$, where α and γ are auxiliary variables, which are saturated to find $f(z)$. This let us derive the conditional pdf given a specific input sequence and the event that an up–crossing occurred.

Prior to transformation, we analyze the conditions for a duration above η. Let γ be the time of the up–crossing and let $\tilde{\gamma} = \gamma + z$ be the time of the adjacent down–crossing, both relative to the sample x_n, i.e. the crossings occur at time $nT_b + \gamma$ and $nT_b + \tilde{\gamma}$. It is known that the samples $x_n, x_{n+1}, \ldots$ are independent, however, the duration may be correlated depending on $\tilde{\gamma}$.

Consider Case A, if $(n+1)T_b < nT_b + \tilde{\gamma} < (n+2)T_b$ (recall that $\tilde{\gamma} > T_b$ for a crossing to be detected), then correlation exists between γ and $\tilde{\gamma}$. The reason for this is, that the up– and down–crossing share the sample x_{n+1} in their expression of the linear approximation of their respective crossing times γ and $\tilde{\gamma}$. Conversely for Case B, if $(n + 2)T_b < nT_b + \tilde{\gamma}$, then the up– and down–crossing do not share any samples. The two cases are described individually in the following, and combined by the marginal pdf $f(z)$ in Section 3.4.

3.3.1. Case A

For a graphical interpretation of the variables used in the transformation, see Fig. 5. Let $a = x_n$, $b = x_{n+1}$, and $c = x_{n+2}$ be the relevant samples to consider on their respective pdfs in the case where the down–crossing is ensured between x_{n+1} and x_{n+2}, and let $f^A(a, b, c)$ be the joint pdf, which, because X_n, X_{n+1} and X_{n+2} are independent is:

$$f^A(a, b, c) = f_{X_n|X_n<\eta}(a)f_{X_{n+1}|X_{n+1}>\eta}(b)f_{X_{n+2}|X_{n+2}<\eta}(c)$$
$$= \frac{f_{X_n}(a)f_{X_{n+1}}(b)f_{X_{n+2}}(c)}{\Pr[X_n < \eta]\Pr[X_{n+1} > \eta]\Pr[X_{n+2} < \eta]},$$

where $f_{X_i}(\cdot)$s are independent Rice pdfs with statistics specified by the mean sequence $\bar{\bar{\mathbf{s}}}$ and noise power N_0. Then the multivariate to multivariate transformation [8] is:

$$f_T^A(\alpha, \gamma, z) = f(a, b, c)|J|,$$

3

where $f_T^A(\alpha, \gamma, z)$ is the transformed pdf and $|J|$ is the absolute determinant of the Jacobian. To ensure a one–to–one mapping between the original pdf and the transformed pdf, it is needed to introduce the variables α and γ which are marginalized later. α and γ can be defined in many different ways to let the mapping be one–to–one, in the following let them have the meaning: $\alpha = a$ is the value of the first sample x_n and γ is the time of the up–crossing relative to x_n.

Let $\gamma' = \gamma + z - T_b$ be the down–crossing time relative to the last sample above η and let the values a, b and c be expressed by the linear approximation using α, γ, and z:

$$a = \alpha, \qquad b = \frac{(\eta - \alpha)T_b}{\gamma} + \alpha,$$

$$c = \frac{\left(\eta - \frac{(\eta - \alpha)T_b}{\gamma} - \alpha\right)T_b}{\gamma'} + \frac{(\eta - \alpha)T_b}{\gamma} + \alpha$$

$$= \frac{(\eta - \alpha)(2\gamma - 2T_b + z)T_b}{\gamma(\gamma + z - T_b)} + \alpha, \qquad (2)$$

where b is found by inserting a in Eqn. (1), and c by inserting b in the same equation, and, given the constraint $(n+1)T_b < nT_b + \tilde{\gamma} < (n+2)T_b$ for Case A, it is known that $a < \eta$, $b > \eta$, and $c < \eta$. The absolute determinant of the Jacobian:

$$|J| = \left| \begin{bmatrix} 1 & 0 & 0 \\ \frac{\partial b}{\partial \alpha} & -\frac{(\eta - \alpha)T_b}{\gamma^2} & 0 \\ \frac{\partial c}{\partial \alpha} & \frac{\partial c}{\partial \gamma} & -\frac{(\eta - \alpha)(\gamma - T_b)T_b}{\gamma(\gamma + z - T_b)^2} \end{bmatrix} \right|$$

$$= \left| \frac{(\eta - \alpha)^2(\gamma - T_b)T_b^2}{\gamma^3(\gamma + z - T_b)^2} \right|$$

and the transformed pdf is:

$$f_T^A(\alpha, \gamma, z) = f^A(a, b, c) \left| \frac{(\eta - \alpha)^2(\gamma - T_b)T_b^2}{\gamma^3(\gamma + z - T_b)^2} \right|,$$

where a, b, and c are the quantities from Eqn. (2). The pdf is now marginalized, and the pdf for Case A is:

$$f^A(z) = \int_{-\infty}^{\eta} \int_{\max[T_b - z, 0]}^{\min[2T_b - z, T_b]} f_T^A(\alpha, \gamma, z) d\gamma d\alpha, \qquad (3)$$

where the integration limits are found in the Appendix.

3.3.2. Case B

Let u be the value where $x_{n+u} > \eta$ is the last sample before the down–crossing, from which it follows that $x_{n+u+1} < \eta$ and $\gamma' = \gamma + z - uT$, and let $a = x_n$, $b = x_{n+1}$, $c = x_{n+u}$ and $d = x_{n+u+1}$ (see Fig. 6), then the pdf:

$$f_u^B(a, b, c, d) = f_{X_n|X_n < \eta}(a) f_{X_{n+1}|X_{n+1} > \eta}(b)$$
$$\cdot f_{X_{n+u}|X_{n+u} > \eta}(c) f_{X_{n+u+1}|X_{n+u+1} < \eta}(d)$$

describes the probability of sample value pairs $\{a, b\}$ and $\{c, d\}$ where the pairs are non–overlapping (definition of Case B).
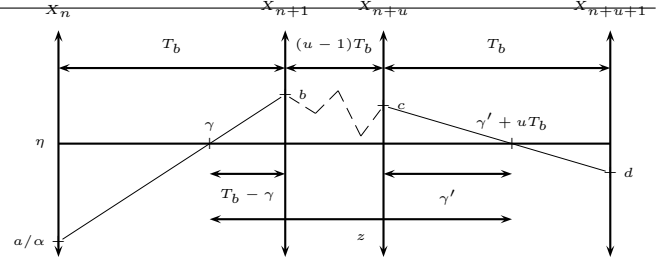
Fig. 6: Linear approximation applied between samples for Case B. The tuple $\{a, b, c, d\}$ consisting of the two pairs $\{a, b\}$ and $\{c, d\}$ depicted is one of the possible pairs yielding the same duration $r = T_b - \gamma + \gamma'$.

Let $r = T_b - \gamma + \gamma'$ be the sum of durations above η in the start– and end–pair so $z = (u-1)T_b + r$. The transformation with auxiliary variables α, β and γ:

$$a = \alpha, \qquad b = \frac{(\eta - \alpha)T_b}{\gamma} + \alpha,$$

$$c = \beta, \qquad d = \frac{(\eta - \beta)T_b}{\gamma'} + \beta = \frac{(\eta - \beta)T_b}{r - T_b + \gamma} + \beta, \qquad (4)$$

and the transformed marginalized pdf is:

$$f_u^B(r) = \int_{-\infty}^{\eta} \int_{\max[T_b - r, 0]}^{\min[2T_b - r, T_b]} \int_{\eta}^{\infty} f_{T,u}^B(\alpha, \gamma, \beta, r) d\beta d\gamma d\alpha, \qquad (5)$$

where a, b, c, d are in Eqn. (4) and the integration limits are found by a similar approach to those in the Appendix.

3.4. Combining Case A and B

Let $N = \lfloor \frac{z}{T_b} \rfloor$ be the minimum number of samples above η. For example, if $N = 0$, i.e. $z < T_b$, one could argue that there could be an up– and down–crossing without it being represented in the samples. However, because of the bandwidth constraints and the sampling synchronization, this is not possible.[1] That is, when $N = 0$, the duration is only represented by Case A, as a duration this short must share the sample x_{n+1}. For $N = 1$, the duration can be represented by both Case A and B, and for $N > 1$ only by Case B.

Let $P_{n+k} = \Pr[X_{n+k} < \eta]$ and $\bar{P}_{n+k} = \Pr[X_{n+k} > \eta]$, then compensating for the model–conditions in Case A and B, and introducing the probability for intermediate samples in Case B to be above η yields the main result:

$$f(z) = f(z|\bar{\mathbf{s}}, X_n < \eta, X_{n+1} > \eta)$$

$$= \begin{cases} P_{n+2} f^A(z) & \text{if } N = 0, \\ P_{n+2} f^A(z) + \bar{P}_{n+2} P_{n+3} f_2^B(z - T_b) & \text{if } N = 1, \\ \prod_{i=2}^{N} (\bar{P}_{n+i}) \big[P_{N+1} f_N^B(z - (N-1)T_b) \\ \quad + \bar{P}_{N+1} P_{N+2} f_{N+1}^B(z - NT_b) \big] & \text{otherwise}, \end{cases}$$

---

[1]This is not absolutely correct as the ripples introduced by the filtering in $p_f(t)$ may lead to unintended up–crossings; this type of error, however, is considered rare and negligible.

where $f^A(z)$ is the one from Eqn. (3) and $f_2^B(r)$ is Eqn. (5) evaluated for $u = 2$ samples above η describing the probability of the remaining duration $r = z - T_b$ — this multiplied with the probability of the intermediate duration $z - r$. $f_N^B(\cdot)$ and $f_{N+1}^B(\cdot)$ is a generalized version of $f_2^B(\cdot)$.

4. CONCLUSION

A probabilistic model for the detector circuit in a tag is presented, allowing further work to derive e.g. Maximum Likelihood receivers. It allows the noise to be correlated between independent sample values of the envelope – this to capture the effect of the natural band–pass filter in the tags antenna. The primary assumption in the work is that the envelope can be approximated by a 1st order linear interpolation between the samples, however, as argued and shown, this approximation results in sufficiently good results. Because of the sample correlation for short durations, the pdf describing the on–duration is piecewise, and no closed form expression for the integrals in each part exist. Future work should include a closed form approximation of the pdf, analysis on the types of symbol errors arising because of the simple detector, or several other uses such as establishing ML detector, determine channel capacity, determine optimal threshold value η, determine optimal symbol durations, etc.

5. REFERENCES

[1] C. Floerkemeier and S. Sarma, "RFIDSim—A Physical and Logical Layer Simulation Engine for Passive RFID," *Transactions on Automation Science and Engineering*, vol. 6, no. 1, pp. 33–43, January 2009.

[2] EPCglobal Inc., *EPC Radio-Frequency Identity Protocols Class-1 Generation-2 UHF RFID Protocol for Communications at 860 MHz - 960 MHz Version 1.2.0*, October 2008.

[3] Daniel M. Dobkin, *The RF in RFID: Passive UHF RFID in Practice*, Newnes, Newton, MA, USA, 2007.

[4] Yifeng Han, Qiang Li, and Hao Min, *System Modelling and Simulation of RFID*, Auto-ID Labs Whitepaper, September 2005.

[5] European Standard (Telecommunications series), *Electromagnetic compatibility and Radio spectrum Matters (ERM); Radio Frequency Identification Equipment operating in the band 865 MHz to 868 MHz with power levels up to 2 W; Part 1: Technical requirements and methods of measurement*, March 2006, V1.1.2, ETSI EN 302 208-1.

[6] A. J. Rainal, "Axis-Crossings of the Phase of Sine Wave Plus Noise," *The Bell System Technical Journal*, vol. 6, no. 4, pp. 737–754, April 1967.

[7] S. O. Rice, "Statistical Properties of a Sine Wave Plus Random Noise," *The Bell System Technical Journal*, vol. 27, no. 1, pp. 109–157, January 1948.

[8] George Casella and Roger L. Berger, *Statistical Interference*, Duxbury, Pacific Grove, CA, USA, 2nd edition, 2002.

6. APPENDIX

The transformed integration limits for α are the same as for a, and:

$$\alpha_{\min} = -\infty, \qquad \alpha_{\max} = \eta$$

For γ, the bounds are found as follows. Using Eqn. (2) it is known that:

for $a < \eta$: $\quad \alpha < \eta, \quad$ for $b > \eta$: $\quad \dfrac{(\eta - \alpha)T_b}{\gamma} > \eta - \alpha \Rightarrow \gamma < T_b,$

for $c < \eta$: $\quad \dfrac{(\eta - \alpha)(2\gamma - 2T_b + z)T_b}{\gamma(\gamma + z - T_b)} < \eta - \alpha$

$$\Rightarrow \dfrac{(2\gamma - 2T_b + z)T_b}{\gamma(\gamma + z - T_b)} < 1.$$

For $c < \eta$, multiply with the denominator on both sides, and consider the two cases (c_1): $\gamma(\gamma + z - T_b) > 0$ and (c_2): $\gamma(\gamma + z - T_b) < 0$, resulting in the following two inequalities, (i_1) and (i_2), respectively:

$$(2\gamma - 2T_b + z)T_b \overset{(i_1)}{\underset{(i_2)}{\lessgtr}} \gamma(\gamma + z - T_b)$$

$$\gamma^2 + \gamma(z - 3T_b) + 2T_b^2 - zT_b \overset{(i_1)}{\underset{(i_2)}{\gtrless}} 0. \qquad (6)$$

For the quadratic function Eqn. (6), the quadratic coefficient is positive, the function is convex, and the roots are $\gamma_1 = 2T_b - z$ and $\gamma_2 = T_b$. From the model, for a crossing to occur, it is known that $0 < \gamma < T_b$, and the two cases are therefore reduced to (c_1') $\gamma + z - T_b > 0$ (or $\gamma > T_b - z$) and (c_2') $\gamma + z - T_b < 0$ (or $\gamma < T_b - z$). First consider the case (c_1'), its inequality (i_1) is satisfied in the interval $\gamma < \min[\gamma_1, \gamma_2]$ or $\gamma > \max[\gamma_1, \gamma_2]$. However, the case is only defined when $\max[T_b - z, 0] < \gamma < T_b$ (from (c_1')), so the interval for (c_1) satisfying the inequality (i_1) is:

$$\max[T_b - z, 0] < \gamma < \min[\gamma_1, \gamma_2].$$

For case (c_2'), the inequality (i_2) is satisfied when $\min[\gamma_1, \gamma_2] < \gamma < \max[\gamma_1, \gamma_2]$. The case is only defined when $0 < \gamma < T_b - z$ (from (c_2')), as $0 < z < 2T_b$ by definition, the case only contributes when $z < T_b$. However, $\min[\gamma_1, \gamma_2]$ for $z < T_b$ is T_b, which is a contradiction as the interval for (c_2) and (i_2) does not overlap and (c_2) is therefore omitted in the bounds of γ. The result follows as:

$$\gamma_{\min} = \max[T_b - z, 0], \qquad \gamma_{\max} = \min[2T_b - z, T_b],$$

which concludes the derivation of the limits.